

# Analyst

Accepted Manuscript



This is an *Accepted Manuscript*, which has been through the Royal Society of Chemistry peer review process and has been accepted for publication.

*Accepted Manuscripts* are published online shortly after acceptance, before technical editing, formatting and proof reading. Using this free service, authors can make their results available to the community, in citable form, before we publish the edited article. We will replace this *Accepted Manuscript* with the edited and formatted *Advance Article* as soon as it is available.

You can find more information about *Accepted Manuscripts* in the [Information for Authors](#).

Please note that technical editing may introduce minor changes to the text and/or graphics, which may alter content. The journal's standard [Terms & Conditions](#) and the [Ethical guidelines](#) still apply. In no event shall the Royal Society of Chemistry be held responsible for any errors or omissions in this *Accepted Manuscript* or any consequences arising from the use of any information it contains.

1  
2  
3 **A turn-on near-infrared fluorescent chemosensor for selective detection of lead**  
4 **ion based on fluophors-gold nanoparticles assembly**  
5  
6  
7  
8  
9  
10

11 **Shaozhen Wang,<sup>\*a</sup> Junyong Sun,<sup>b</sup> and Feng Gao<sup>\*b</sup>**

12 *<sup>a</sup>Department of Pharmacy, Wannan Medical College, Wuhu 241002, P. R. China.*

13 *E-mail:shaozhenwang@hotmail.com.*

14 *<sup>b</sup>Anhui Key Laboratory of Chemo/Biosensing, College of Chemistry and Materials Science, Anhui*

15 *Normal University, Wuhu 241000, P. R. China. E-mail:fgao@mail.ahnu.edu.cn.*

16  
17  
18  
19  
20  
21  
22  
23  
24  
25  
26  
27  
28  
29  
30  
31  
32  
33  
34  
35  
36  
37  
38  
39  
40  
41  
42  
43  
44  
45  
46  
47  
48  
49  
50  
51  
52  
53  
54  
55  
56  
57  
58  
59  
60  
  
\*To whom correspondence should be addressed.

## Abstract

A turn-on fluorescent chemosensor of  $\text{Pb}^{2+}$  in near-infrared(NIR) region, which is based on the  $\text{Pb}^{2+}$ -tuned restored fluorescence of a weakly fluorescent fluophors-gold nanoparticles (AuNPs) assembly, has been reported. In this fluophors-AuNPs assembly, NIR fluorescent dye brilliant cresyl blue (BCB) molecules act as fluophors and are used for signal transduction of fluorescence, while AuNPs act as quenchers to quench the nearby fluorescent BCB molecules via electron transfer. In the presence of  $\text{Pb}^{2+}$ , fluorescent BCB molecules detached from AuNPs and restored their fluorescence due to the formation of chelating complex between  $\text{Pb}^{2+}$  and glutathione confined on AuNPs. Under the optimal conditions, the present BCB-AuNPs assembly is capable of detecting  $\text{Pb}^{2+}$  with a concentration ranging from  $7.5 \times 10^{-10}$  to  $1 \times 10^{-8}$  mol  $\text{L}^{-1}$  ( $0.16$ - $2.1$  ng  $\text{mL}^{-1}$ ) and a detection limit of  $0.51$ nM ( $0.11$  ng  $\text{mL}^{-1}$ ). The present BCB-AuNPs assembly can be used in aqueous media for the determination of  $\text{Pb}^{2+}$  unlike common organic fluorescent reagent, and also shows advantages of NIR fluorescence spectrophotometry such as less interference, lower detection limit, and higher sensitivity. Moreover, the present method was successfully applied to the detection of  $\text{Pb}^{2+}$  in water samples with satisfactory results.

## Introduction

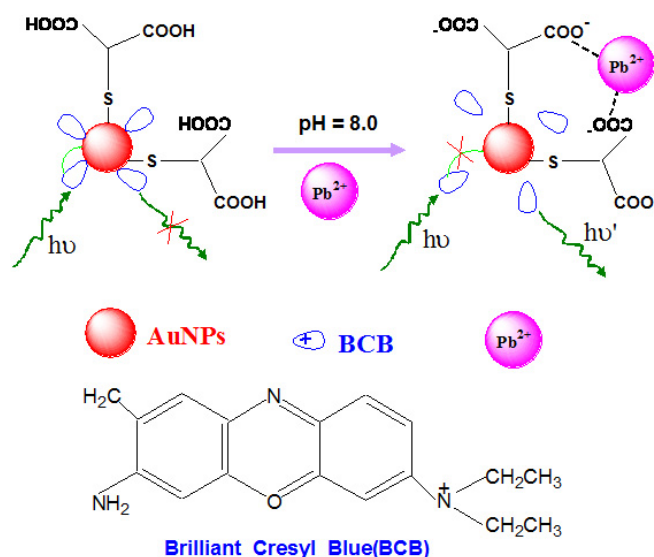
Lead ion ( $\text{Pb}^{2+}$ ), generally regarded as one of the very abundant and toxic heavy metal ions in environment pollutant, is not biodegradable, and therefore easily accumulated in the environments, which leads to the contamination of soil, water, and food.<sup>1-3</sup> The relevant studies have demonstrated that the long accumulation of  $\text{Pb}^{2+}$  in the body is hazardous to both the central and peripheral nervous systems, and may cause many serious diseases such as muscle paralysis, memory loss, hepatic injury, lung damage, and hypertension, and so on.<sup>1-5</sup> For example, non-adults may suffer from permanent neurological damages, behavioral dysfunctions, and decreased IQs even at blood lead level as low as 100 ppb or 500 nM because of the non-degradation of lead ions.<sup>1-5</sup> In our daily lives, the main sources of lead pollution are attributed to the widespread employments and their auto-release of lead-containing products include coal combustion, gasoline, paints used in water supply systems, and lead-acid batteries.<sup>1-5</sup> As a result, it is of great interest to develop sensitive and reliable methods for detecting  $\text{Pb}^{2+}$  in real samples such as water, human blood, and soil.

Up to now, different classic approaches have been developed for the determination of  $\text{Pb}^{2+}$  such as inductively coupled plasma mass spectrometry (ICP-MS),<sup>6,7</sup> liquid-phase micro-extraction with atomic absorption spectroscopy,<sup>8</sup> functional nucleic acids (*e.g.* DNazymes, aptamers)-based sensors,<sup>1,9</sup> dynamic light scattering technique,<sup>10,11</sup> electrochemical methods,<sup>12-19</sup> and optical methods including fluorimetric methods,<sup>20-33</sup> visual detection,<sup>34</sup> UV-vis spectrophotometry,<sup>3</sup> chemiluminescence,<sup>36</sup> and photonic crystal optrode.<sup>37</sup> Among these developed approaches, fluorescence-based methods have shown great advantages such as high sensitivity, simple instrumentation, and easy operation.<sup>20-33</sup> Fluorescence-based spectroscopy in the near-infrared (NIR) region, in which fluorescence emission generally occurs above 650 nm, is an attractive area because NIR fluorescence shows some advantages over visible-region fluorescence such as minimized background spectra interference and reduced interfering from Raman and Rayleigh scattering lights.<sup>38-40</sup> Obviously, based on NIR fluorescence spectroscopy, enhanced sensitivity for analytical

1  
2  
3 assay can be expected. For example, Wang group recently has reported different NaYF<sub>4</sub>-based  
4  
5  
6  
7  
8  
9  
10  
11  
12  
13  
14  
15  
16  
17  
18  
19  
20  
21  
22  
23  
24  
25  
26  
27  
28  
29  
30  
31  
32  
33  
34  
35  
36  
37  
38  
39  
40  
41  
42  
43  
44  
45  
46  
47  
48  
49  
50  
51  
52  
53  
54  
55  
56  
57  
58  
59  
60  
assay can be expected. For example, Wang group recently has reported different NaYF<sub>4</sub>-based  
nanomaterials with NIR irradiation for assays of different analytes such as explosives, glucose, and  
hydrogen peroxide, demonstrating that NIR fluorescence methods show many advantages including  
no auto-fluorescence, low damage to samples, no photobleaching, and high sensitivity.<sup>41-45</sup>  
However, determination of Pb<sup>2+</sup> with NIR fluorescence photospectroscopy has rarely been  
reported.<sup>32,33</sup>

In present study, a novel efficient NIR fluorescent chemosensor based on weakly fluorescent  
fluophors-gold nanoparticles (AuNPs) assembly has been developed for the determination of Pb<sup>2+</sup> in  
aqueous solutions (Scheme 1). In this fluophors-AuNPs assembly, commercially available NIR  
fluorescent dye brilliant cresyl blue (BCB) molecules act as fluophors and used for signal  
transduction, while AuNPs act as quenchers to quench the BCB fluorescence. As shown in Scheme  
1, at pH 8.0, positively charged BCB molecules are self-assembled on negatively charged glutathione  
(GSH)-modified AuNPs via electrostatic interaction or Au-N bond interaction<sup>40</sup>, which induces  
fluorescence quenching(turn-off) of BCB as a result of strong quenching ability of AuNPs to nearby  
fluophors.<sup>40, 46-50</sup> The fluorescence of BCB switches to “turn-on” (restore) upon addition of Pb<sup>2+</sup> due  
to the coordination interactions between COO<sup>-</sup> group of the GSH and Pb<sup>2+</sup> to form chelating  
complex,<sup>51</sup> which leads the dissociation of BCB molecules from the surfaces of AuNPs and thus  
their fluorescence restore. Based on the restored fluorescence, a homogenous assay method for Pb<sup>2+</sup>  
is proposed and the feasibility of the AuNPs-based “turn-on” fluorescence sensing for Pb<sup>2+</sup> is  
demonstrated. Herein, BCB and AuNPs were chosen to construct weakly fluorescent( *i.e.*, low  
background) assembly which is desirable for sensitive turn-on assay are based on the two facts,  
BCB is water soluble, commercially available, and NIR fluorescent emission. In addition, AuNPs  
have displayed strong quenching ability to nearby fluophors through different mechanisms<sup>40,52-55</sup>  
because AuNPs processes a broad absorption band and have high extinction coefficients (*e.g.* up to  
 $8 \times 10^8 \text{ L mol}^{-1} \text{ cm}^{-1}$  for 13 nm AuNPs at 520 nm),<sup>53-57</sup> which is about 3-5 orders of magnitude higher

than common organic molecules.<sup>48,57</sup> These distinguished properties of BCB and AuNPs allow BCB-AuNPs assembly to form low background fluorescence for turn-on detect with enhanced sensitivity. In addition, the high water solubility of BCB-AuNPs assembly enables the assay to be performed in aqueous media without the need for organic cosolvents. As a result, the quantitative analysis of  $\text{Pb}^{2+}$  can be realized in a simple and sensitive approach.



Scheme 1. Illustration of FET-based sensor of lead ion

## Experimental

### Instrumentation

An LS-55 fluorescence spectrophotometer (PerkinElmer, USA) combined with a quartz cell (1 cm × 1 cm) was employed for fluorescence spectra measurements. UV-Vis absorption spectra were performed on a UV-3010 spectrophotometer (Hitachi, Japan). A Hitachi H-600 transmission electron microscopy (TEM) (Tokyo, Japan) was used for the morphological characterization of the prepared Au nanoparticles.

### Materials

Chloroauric acid tetrahydrate ( $\text{HAuCl}_4 \cdot 4\text{H}_2\text{O}$ ) was purchased from Aladdin-Reagent Company. Trisodium citrate, brilliant gresyl blue, glutathione (GSH), and lead nitrate ( $\text{Pb}(\text{NO}_3)_2$ ) were

1  
2  
3 obtained from Sinopharm Chemical Reagent Co., Ltd (Shanghai, China). The buffer solution (pH  
4 6.0-8.5) was prepared by 0.01 mol L<sup>-1</sup> KH<sub>2</sub>PO<sub>4</sub>-Na<sub>2</sub>HPO<sub>4</sub>. The reagents used in this study were of  
5 analytical grade and used without any further purification. All solutions were prepared with Milli-Q  
6 purified water (>18.0 MQ) was used throughout for the preparation of solutions.  
7  
8  
9  
10  
11

### 12 **AuNPs preparation and surface modification with GSH**

13  
14  
15 In this study, AuNPs were prepared with HAuCl<sub>4</sub> reduction by trisodium citrate, as described in  
16 previous reports<sup>53-55</sup>. Typically, into a round-bottom flask with a reflux condenser, 99.0 mL water  
17 and 1.0 mL 1% HAuCl<sub>4</sub> solution were injected under vigorous stirring, and the flask was then  
18 incubated in oil bath to reflux under stirring. While the mixture was heated to boiling state, 5.0 mL  
19 of trisodium citrate solution (1%, weight percent) was quickly injected into the flask, and then the  
20 reaction was allowed to reflux for 20 min. The color of the solution was turned to deep red from  
21 pale yellow and the solution was cooled to room temperature and then stored at 4°C in the  
22 refrigerator for further use.  
23  
24  
25  
26  
27  
28  
29  
30  
31  
32  
33

34 The surface modification of AuNPs with GSH was also carried out according to previous  
35 literature.<sup>53</sup> In general, an aqueous solution of gold nanoparticle (4.0 nM) and GSH (1.0 μM) were  
36 mixed in the volume ratio of 8:1, and then pH of the resulting mixture was adjusted to 9.0 using 1.0  
37 M NaOH. The mixture was let to react for 3 h at room temperature in dark condition under  
38 continuing stirring to ensure GSH confined onto the surface of AuNPs.  
39  
40  
41  
42  
43  
44

### 45 **Preparation of BCB-AuNPs assembly**

46  
47  
48 To investigate the behavior of fluorescence quenching of BCB by AuNPs, different concentration  
49 of AuNPs was added into the 200 μL BCB solution (100 μM) with a pH value of 8.0. The final  
50 volume of the mixture solution was adjusted to 2.0 mL with phosphate buffer solution (pH 8.0).  
51 Then the solution was equilibrated at ambient temperature for 30 min, and the fluorescence of the  
52 mixture solutions were measured at 660 nm with an excitation at 520 nm.  
53  
54  
55  
56  
57  
58  
59

### 60 **Procedures for the determination of Pb<sup>2+</sup>**

1  
2  
3 For the determination of  $\text{Pb}^{2+}$ , a mixture solution containing 200  $\mu\text{L}$  of BCB solution (100  $\mu\text{M}$ )  
4 and 850  $\mu\text{L}$  of AuNPs (4.0 nM) was added into in a series of 10 mL volumetric flasks, and then  
5  
6  
7  
8 various concentrations of  $\text{Pb}^{2+}$  solution were added, then the mixture was diluted to 2.0 mL with pH  
9  
10 8.0 phosphate buffer. The mixture was allowed to react thoroughly for 40 min at room temperature.  
11  
12  
13 The fluorescence intensities of the mixture solutions were measured at 660 nm with an excitation at  
14  
15 520 nm.  
16  
17  
18  
19

## 20 **Results and discussion**

### 21 **Characterization of AuNPs**

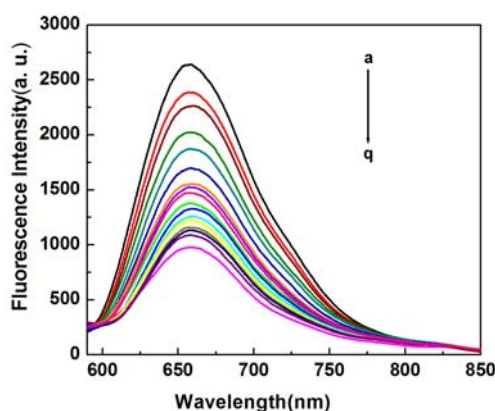
22  
23  
24  
25 The typical TEM images of the as-prepared AuNPs are shown in Fig. S1 (Supporting  
26  
27 Information). We can see that the shape of AuNPs are regular, monodisperse, and spherical, and the  
28  
29 average diameter of AuNPs is about  $13.0 \pm 1.3$  nm. A characteristic surface plasmon resonance (SPR)  
30  
31 peak is located at 520 nm,<sup>53-55</sup> as shown in UV-vis absorption spectra (Fig. S2, curve a, Supporting  
32  
33 Information). Based on the Beer's law ( $A = \epsilon bc$ ), and the extinction coefficient ( $\epsilon$ ) of  $2.01 \times 10^8 \text{ M}^{-1}$   
34  
35  $\text{cm}^{-1}$  for about 13 nm AuNPs at 520 nm,<sup>48,52-55</sup> the particle concentration of the AuNPs solution was  
36  
37 estimated to be 4.0 nM. After the modification of GSH on AuNPs, the characteristic SPR peak is  
38  
39 slight red-shifting and located at 522 nm (Fig. S2, curve b, Supporting Information), suggesting the  
40  
41 AuNPs are successfully modified by GSH through the Au-S covalent bond.<sup>58</sup>  
42  
43  
44  
45  
46  
47  
48

### 49 **Fluorescence quenching of BCB by AuNPs**

50  
51 The quenching effect of AuNPs on fluorescence of BCB was studied. Fig. 1 displays the emission  
52  
53 spectra of BCB in presence of different concentrations of AuNPs. As shown in this figure, in the  
54  
55 absence of AuNPs, BCB solution fixed at a concentration of 10  $\mu\text{M}$  shows the characteristic  
56  
57 emission fluorescence at ca. 660 nm,<sup>59</sup> while different concentrations of AuNPs ranging from 0.1 to  
58  
59 1.7 nM were introduced into BCB solution, the fluorescence of BCB at maximum emission were  
60



1  
2  
3  
4 quenched gradually with the increasing of concentration of AuNPs, accompanying with a very  
5  
6 slight 3 nm red-shifting. In addition, when the added AuNPs was above 1.7 nM, the fluorescence  
7  
8 intensity did not show obvious change, indicating the quenching of BCB reached at the maximum  
9  
10 level. The maximum quenching efficiency can be calculated to be 75.1% on the basis of the  
11  
12 formular,  $E_q=1-F/F_0$ , where  $F_0$  and  $F$  represent the fluorescence intensity in the absence and  
13  
14 presence of AuNPs, respectively. This result suggests that AuNPs shows strong quenching ability to  
15  
16 the fluorescence of BCB. The spectroscopy of BCB-AuNPs assembly showed a good stability in  
17  
18 aqueous solution for over one week. Furthermore, TEM measurements (not shown) further  
19  
20 demonstrated that the morphology of AuNPs did not shown discernable change upon BCB  
21  
22 molecules were confined on AuNPs surface. As demonstrated by the negligible changes of the  
23  
24 fluorescence signal and morphology of BCB-AuNPs assembly, we believe the BCB-AuNPs  
25  
26 assembly is favorable for their further analytical applications.  
27  
28  
29  
30  
31  
32



33  
34  
35  
36  
37  
38  
39  
40  
41  
42  
43  
44  
45  
46  
47  
48 **Fig. 1** The fluorescence spectra of BCB in the BCB-AuNPs system with various concentrations of  
49  
50 AuNPs in phosphate buffer with a pH of 8.0. BCB:10  $\mu$ M; AuNPs (from a to q): 0, 0.1, 0.2, 0.3, 0.4,  
51  
52 0.5, 0.6, 0.8, 0.9, 1.0, 1.1, 1.2, 1.3, 1.4, 1.5, 1.6, 1.7 nM.  
53  
54  
55

56  
57 Previous studies have demonstrated that three typical mechanisms including fluorescence  
58  
59 resonance energy transfer (FRET),<sup>53-56</sup> electron transfer (ET),<sup>40</sup> and inner filter effect (IFE)<sup>5-</sup>  
60  
dominate the fluorescence quenching of fluorophores by the nearby AuNPs. In this study, as shown

1  
2  
3 in Fig. S3(Supporting Information), only slight overlap between the emission spectrum of BCB and  
4  
5 the absorption spectrum of AuNPs was observed, the observed dramatic quenching of BCB is less  
6  
7 likely caused by energy transfer.<sup>40, 60-62</sup> In addition, as shown in Fig.1, the observed spectral changes  
8  
9 of BCB in the presence of various concentrations of AuNPs with 3-nm red-shift of the emission  
10  
11 maximum, suggested that AuNPs quenched the fluorescence of adsorbed BCB more likely through  
12  
13 electron transfer rather than energy transfer processes.<sup>40,46,63</sup> Besides, the IFE may also contribute to  
14  
15 the fluorescence quenching of BCB, but generally the contribution of IFE to quenching of fluophors  
16  
17 is subordinate to FRET or ET.<sup>64</sup> In this study, electron transfer mechanism may dominate the  
18  
19 quenching of BCB by nearby AuNPs.  
20  
21  
22  
23  
24  
25  
26

### 27 **Fluorescence turn-on assay of Pb<sup>2+</sup> with BCB-AuNPs assembly**

28  
29 Fig. 2 depicts the emission spectra of BCB, BCB-Pb<sup>2+</sup>, BCB-AuNPs, and BCB-AuNPs-Pb<sup>2+</sup>,  
30  
31 respectively, under the same experimental conditions. As shown in this figure, BCB solution  
32  
33 exhibits a strong fluorescence signal at about 660 nm (curve a). When different concentrations of  
34  
35 Pb<sup>2+</sup> were added to the solution, the fluorescence intensity and peak location did not show any  
36  
37 obvious changes (curve b, curve c), indicating that there is no interaction between Pb<sup>2+</sup> and BCB.  
38  
39 Also shown in this figure, upon AuNPs was added into the BCB solution, the fluorescence intensity  
40  
41 of BCB was decreased dramatically (curve d) via electron transfer between BCB molecules and  
42  
43 AuNPs. At pH 8.0, BCB molecules are positively charged<sup>59</sup> and GSH-modified AuNPs are  
44  
45 negatively charged,<sup>51</sup> and therefore there exists the electrostatic interaction between them. On the  
46  
47 other hand, the -NH<sub>2</sub> group contained in BCB molecules can react with gold.<sup>40</sup> We assumed that the  
48  
49 electrostatic interaction and Au-N interaction result in the formation of BCB-AuNPs assembly.  
50  
51 More interesting, when Pb<sup>2+</sup> ions were introduced into the BCB-AuNPs assembly solution, the  
52  
53 fluorescence of BCB was restored (curve e and f ), suggesting that BCB molecules released from  
54  
55 the surfaces of AuNPs due to the formation of chelating complex between Pb<sup>2+</sup> and the COO<sup>-</sup> of the  
56  
57  
58  
59  
60

GSH.<sup>51</sup>

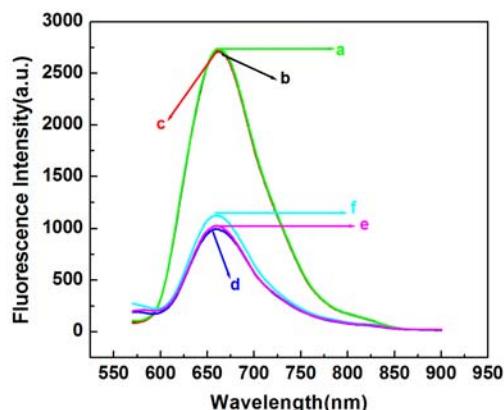


**Fig. 2** Fluorescence spectra of (a) 10  $\mu\text{M}$  BCB, (b) (a) + 0.25 nM  $\text{Pb}^{2+}$ , (c) (a) + 2.5 nM  $\text{Pb}^{2+}$ , (d) (a) + 1.7 nM AuNPs, (e) (d) + 0.25 nM  $\text{Pb}^{2+}$ , and (f) (d) + 2.5 nM  $\text{Pb}^{2+}$  in phosphate buffer with a pH of 8.0.

### Optimization of experiment conditions for $\text{Pb}^{2+}$ assay

The effect of pH on the BCB-AuNPs assembly was investigated. Fig. 3 displays the fluorescence difference ( $\Delta F$ ) of the BCB-AuNPs assembly solution in absence and presence of  $\text{Pb}^{2+}$  in the pH range from 6.0 to 8.5. As shown in this figure, it can be seen that the largest fluorescence difference is obtained at pH 8.0. As aforementioned, at pH 8.0, BCB molecules are positively charged,<sup>59</sup> while GSH-AuNPs are negatively charged,<sup>51</sup> and thus the strong electrostatic interaction between them is favorable to form compact BCB-AuNPs assembly and therefore transfer electrons between BCB molecules and AuNPs, resulting in the lowest background fluorescence of the BCB-AuNPs assembly. In addition, the negatively charged  $-\text{COO}^-$  groups of GSH confined on AuNPs easily bind strongly with  $\text{Pb}^{2+}$ , leading to releasing of BCB molecules from GSH-AuNPs surface and therefore the restoration of their fluorescence. Combining these two points for considering, it is not surprising that the maximum fluorescence difference can be obtained at pH 8.0. Therefore, pH 8.0 buffer was recommended and used throughout in this study.

At room temperature, when BCB and AuNPs were mixed, the relative fluorescence intensity

reached a stable value within 30 min. In addition, upon  $\text{Pb}^{2+}$  was introduced into BCB-AuNPs assembly solution, the fluorescence was restored quickly and reach a stable value within 7 min. In this study, a incubation time of 40 min was adopted for  $\text{Pb}^{2+}$  assay.

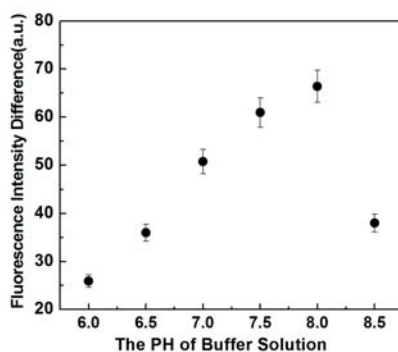


**Fig. 3** Effect of pH of buffer solution on the fluorescent enhancement efficiency of the BCB-AuNPs system in the presence of  $\text{Pb}^{2+}$ . The concentrations of BCB, AuNPs and  $\text{Pb}^{2+}$  are 10  $\mu\text{M}$  BCB, 1.7 nM and 1.5 nM, respectively.

### NIR fluorescent detection $\text{Pb}^{2+}$ with BCB-AuNPs assembly

Under the optimum conditions, the proposed BCB-AuNPs assembly system for the determination of  $\text{Pb}^{2+}$  was evaluated. Fig. 4 displays the fluorescence spectra of BCB-AuNPs assembly system in the presence of different concentrations of  $\text{Pb}^{2+}$ . As shown in this figure, the fluorescence intensity of BCB-AuNPs restored gradually with the increasing of concentrations of  $\text{Pb}^{2+}$ , indicating that more  $\text{Pb}^{2+}$  was added, the more BCB molecules were released from the surface of AuNPs and as thus the fluorescence was restored gradually. The plot of the relatively enhanced fluorescence intensity,  $\Delta F = F - F_0$ , against the concentration of added  $\text{Pb}^{2+}$  is shown in Fig 4. Herein,  $F$  and  $F_0$  represent the fluorescence intensity in the presence of different concentrations of  $\text{Pb}^{2+}$  and absence of  $\text{Pb}^{2+}$ , respectively. It is clear that the enhanced fluorescence intensity ( $\Delta F$ ) exhibits a linear response to  $\text{Pb}^{2+}$  concentration in the range of  $7.5 \times 10^{-10}$ - $1.0 \times 10^{-8}$  M (0.16-2.1 ng mL<sup>-1</sup>) with a correlation coefficient of 0.998. The limit of detection ( $3\sigma$ ) for  $\text{Pb}^{2+}$  is 0.51 nM (0.11 ng mL<sup>-1</sup>).

Where  $\sigma$  represents the standard deviation of eight blank measurements. These analytical parameters are better than or comparable to those reported in literatures, as shown in Table S1(Supporting Information). The reproducibility of the present system was also evaluated by measurements of 5.0 nM  $\text{Pb}^{2+}$  and the relative standard deviation (RSD) for 11 repeated measurements was found to be 1.93%, indicating that the response of the BCB-AuNPs assembly system to  $\text{Pb}^{2+}$  assay is highly reproducible.

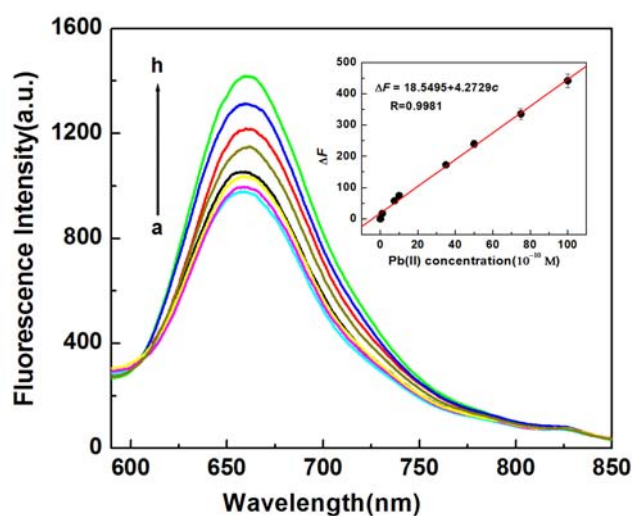


**Fig. 4** Fluorescence spectra of BCB-AuNPs system in presence of different concentrations of  $\text{Pb}^{2+}$  (From a to i: 0,  $1 \times 10^{-10}$ ,  $7.5 \times 10^{-10}$ ,  $1 \times 10^{-9}$ ,  $3.5 \times 10^{-9}$ ,  $5 \times 10^{-9}$ ,  $7.5 \times 10^{-9}$ ,  $1 \times 10^{-8}$  M). Inset: the enhanced fluorescence intensities as a function of concentration of  $\text{Pb}^{2+}$ . BCB:10  $\mu\text{M}$ , AuNPs: 1.7 nM, pH=8.0.

#### Analysis of $\text{Pb}^{2+}$ in Real samples with the proposed BCB-AuNPs assembly system

Prior to assaying  $\text{Pb}^{2+}$  in real samples, the effect of potential interfering substances such as coexistence of common ions on the determination of  $\text{Pb}^{2+}$  was investigated. We examined the fluorescence response of the present system to  $\text{Pb}^{2+}$  at a concentration of 5.0 nM in the presence of different interfering substances. The effects of main relevant metal ions on the fluorescence intensity of the present system for 5 nM  $\text{Pb}^{2+}$  were studied and the results showed that the potential

coexisted ions induced less than  $\pm 5\%$  interference with the detection of the  $\text{Pb}^{2+}$  (Table S2, Supporting Information). These results suggested that BCB-AuNPs system possessed a good selective fluorescence response toward  $\text{Pb}^{2+}$ , and also indicated that a turn-on fluorescent method for the determination of  $\text{Pb}^{2+}$  could be developed by the present system.

To evaluate the applicability of the method, we use this method to detect real different samples. Certain amounts of  $\text{Pb}^{2+}$  standard solution were directly spiked into the real samples, and the results of real samples by standard addition method are summarized in Table 1. As shown in Table 1, excellent recoveries in the range from 95.0% to 114.0% were obtained for all samples, and the results are also good agreements with classical ICP-AAS method, suggesting that the proposed method is reliable and suitable for real applications.

**Table 1.** Results of determination of  $\text{Pb}^{2+}$  in real samples<sup>a</sup>

	The proposed method				ICP-AAS			
	Original (Mean $\pm$ SD) / ng mL <sup>-1</sup>	Spiked / ng mL <sup>-1</sup>	Found (Mean $\pm$ SD) / ng mL <sup>-1</sup>	Recovery (Mean $\pm$ SD) / %	Original (Mean $\pm$ SD) / ng mL <sup>-1</sup>	Spiked / ng mL <sup>-1</sup>	Found (Mean $\pm$ SD) / ng mL <sup>-1</sup>	Recovery (Mean $\pm$ SD) / %
Waste water (form dye mill)	1.61 $\pm$ 0.03	0.2	1.80 $\pm$ 0.01	95.0 $\pm$ 5.0	1.59 $\pm$ 0.01	0.2	1.78 $\pm$ 0.01	95.0 $\pm$ 0.0
		0.3	1.93 $\pm$ 0.02	106.6 $\pm$ 6.7		0.3	1.90 $\pm$ 0.02	103.3 $\pm$ 3.3
		0.5	1.30 $\pm$ 0.01	114.0 $\pm$ 2.0		0.5	1.25 $\pm$ 0.03	116.0 $\pm$ 0.0
Tap water	0.73 $\pm$ 0.04	1.0	1.68 $\pm$ 0.03	95.0 $\pm$ 3.0	0.67 $\pm$ 0.03	1.0	1.62 $\pm$ 0.02	95.0 $\pm$ 1.0

<sup>a</sup> all the data are the mean for five repeated measurements

## Conclusions

In summary, we have developed a convenient turn-on NIR fluorescent method for sensitive detection of  $\text{Pb}^{2+}$  with the BCB-AuNPs assembly in aqueous solutions. Based on the chelating interaction between  $\text{Pb}^{2+}$  and  $-\text{COO}^-$  groups confined on the surface of AuNPs, the BCB molecules release from the BCB-AuNPs assembly and therefore their fluorescence restore. By virtue of the restored fluorescence, a turn-on type fluorescent chemosensor for  $\text{Pb}^{2+}$  was developed. The

1  
2  
3 proposed method was successfully applied to the determination of Pb<sup>2+</sup> in different water samples  
4  
5 including waste water and tap water, suggesting the present method has the potentially practical  
6  
7 applications in environmental analysis.  
8  
9

## 10 11 12 13 **Acknowledgements**

14  
15  
16 S. Wang thanks the Natural Science Foundation of China (Grant No. 21301008) for the financial  
17  
18 support. F. Gao is grateful for the financial supports from the Natural Science Foundation of China  
19  
20 (Grant No. 21175002, 21055001), Program for New Century Excellent Talents in University  
21  
22 (NCET-12-0599), Anhui Provincial Natural Science Foundation for Distinguished Youth (Grant No  
23  
24 1108085J09), and the project sponsored by SRF for ROCS, SEM.  
25  
26  
27  
28  
29

## 30 31 **References**

- 32  
33 1 G. Zhu and C. Zhang, *Analyst*, 2014, **139**, 6326-6342.  
34  
35 2 H. N. Kim, W. X. Ren, J. S. Kim, and J. Yoon, *Chem. Soc. Rev.*, 2012, **41**, 3210-3244.  
36  
37 3 Y.W. Lin, C. C. Huang, and H.T. Chang, *Analyst*, 2011, **136**, 863-871.  
38  
39 4 G. Aragay, J. Pons, and A. Merkoci, *Chem. Rev.*, 2011, **111**, 3433-3458.  
40  
41 5 K. Steenland, and P. Boffetta, *Am. J. Ind. Med.*, 2000, **38**, 295-299.  
42  
43 6 H. F. Hsieh, W. S. Chang, Y. K. Hsieh, and C. F. Wang, *Talanta*, 2009, **79**, 183-188.  
44  
45 7 G. Grindlay, J. Mora, L. Gras, and M.T.C. de Loos-Vollebregt, *Anal. Chim. Acta*, 2009,  
46  
47 **652**, 154-160.  
48  
49 8 R. E. Rivas, I. L. Garclá, and M. H. Cordoba, *Anal. Methods*, 2010, **2**, 225-230.  
50  
51 9 D. D. Nie, H. Y. Wu, and Q. S. Zheng, et al., *Chem. Commun.*, 2012, **48**, 1150-1152.  
52  
53 10 X. M. Miao, L. S. Ling, and X.T. Shuai, *Chem. Commun.*, 2011, **47**, 4192-4194.  
54  
55 11 L. Beqa, A. K. Singh, S. A. Khan, and D. Senapati, et al., *ACS Appl. Mater. Interfaces*, 2011, **3**,  
56  
57 668-673.  
58  
59  
60



- 1  
2  
3 12 M. Guziński, G. Lisak, J. Kupis, and A. Jasiński, et al., *Anal. Chim. Acta*, 2013, **791**, 1-12.  
4  
5 13 V. Meucci, S. Laschi, M. Minunni, and C. Pretti, et al., *Talanta*, 2009, **77**, 1143-1148.  
6  
7 14 Y. Wang, Z. Q. Liu, X. Y. Hu, and J. L. Cao, et al., *Talanta*, 2009, **77**, 1203-1207.  
8  
9 15 O. E. Tall, N. J. Renault, M. Sigaud, and O. Vittori, *Electroanalysis*, 2007, **19**, 1152-1159.  
10  
11 16 G. Li, Z. M. Ji, and K. B. Wu, *Anal. Chim. Acta*, 2006, **577**, 178-182.  
12  
13 17 B. Wang, B. Luo, M. H. Liang, and A. Wang, et al., *Nanoscale*, 2011, **3**, 5059-5066.  
14  
15 18 X. R. Yang, J. Xu, X. M. Tang, and H. X. Liu, et al., *Chem. Commun.*, 2010, **46**, 3107-3109.  
16  
17 19 J. A. Rodriguez, I. S. Ibarra, C. A. Galan-Vidal, and M. Vega, et al., *Electroanalysis*, 2009,  
18  
19 **21**, 452-458.  
20  
21 20 X. H. Zhao, R. M. Kong, X. B. Zhang, and H. M. Meng, et al., *Anal. Chem.*, 2011, **83**,  
22  
23 5062-5066.  
24  
25 21 C. L. Li, K. T. Liu, Y. W. Lin, and H. T. Chang, *Anal. Chem.*, 2011, **83**, 225-230.  
26  
27 22 E. M. Ali, Y. G. Zheng, H. H. Yu, and J. Y. Ying, *Anal. Chem.*, 2007, **79**, 9452-9458.  
28  
29 23 X. Wang, and X. Q. Guo, *Analyst*, 2009, **134**, 1348-1354.  
30  
31 24 J. J. Yao, J. S. Li, J. Owens, and W. W. Zhong, *Analyst*, 2011, **136**, 764-768.  
32  
33 25 M. Y. Liu, X. H. Lou, J. Du, and M. Guan, et al., *Analyst*, 2012, **137**, 70-72.  
34  
35 26 L. Wang, Y. Jin, J. Deng, and G. Z. Chen, *Analyst*, 2011, **136**, 5169-5174.  
36  
37 27 Z. Q. Hu, C. S. Lin, X. M. Wang, and L. Ding, et al., *Chem. Commun.*, 2010, **46**, 3765-3767.  
38  
39 28 T. Li, S. J. Dong, and E. K. Wang, *J. Am. Chem. Soc.*, 2010, **132**, 13156-13157.  
40  
41 29 Y. Xiang, A. J. Tong, and Y. Lu, *J. Am. Chem. Soc.*, 2009, **131**, 15352-15357.  
42  
43 30 A. K. Tyagi, J. S. Ramkumar, and O. D. Jayakumar, *Analyst*, 2012, **137**, 760-764.  
44  
45 31 H. Y. Ju, M. H. Lee, J. Kim, and J. S. Kim, et al., *Talanta*, 2011, **83**, 1359-1363.  
46  
47 32 J. Wu, and Y. Qin, *Sens. Actuators B*, 2014, **192**, 51-55.  
48  
49 33 S. Xu, S. Xu, Y. Zhu, and W. Xu, et al., *Nanoscale*, 2014, **6**, 12573-12579.  
50  
51 34 H. Zhu, T. Yu, H. Xu, K. Zhang, H. Jiang, Z. Zhang, Z. Wang, S. Wang, *ACS Appl. Mater.*  
52  
53  
54  
55  
56  
57  
58  
59  
60



- 1  
2  
3  
4  
5  
6  
7  
8  
9  
10  
11  
12  
13  
14  
15  
16  
17  
18  
19  
20  
21  
22  
23  
24  
25  
26  
27  
28  
29  
30  
31  
32  
33  
34  
35  
36  
37  
38  
39  
40  
41  
42  
43  
44  
45  
46  
47  
48  
49  
50  
51  
52  
53  
54  
55  
56  
57  
58  
59  
60
- Interfaces*, 2014, **6**, 21461-21467.
- 35 Y. Wang, J. Wang, F. Yang, and X. R Yang, *Microchim Acta*, 2010, **171**,195-201.
- 36 J. Elbaz, B. Shlyahovsky, and I. Willner, *Chem. Commun.*, 2008, **44**,1569-1571.
- 37 C. E. Reese and S. A. Asher, *Anal Chem.*, 2003, **75**, 3915-3918.
- 38 M. Sun, H. Yu, H. Zhu, F. Ma, S. Zhang, D. Huang, S. Wang, *Anal. Chem.*, 2014, **86**, 671-677.
- 39 J. Rao, A. Dragulescu-Andrasi, and H. Yao, *Curr. Opin. Biotechnol.*, 2007, **18**, 17-25.
- 40 L. Shang, J. Yin, J. Li, L. Jin, and S. Dong, *Biosens. Bioelectron.*, 2009, **25**, 269-274.
- 41 Y. Ma, S. Huang, M. Deng, L. Wang. *ACS Appl. Mater. Interfaces*, 2014, **6**, 7790-7796.
- 42 J. Liu, L. Lu, A. Li, J. Tang, S. Wang, S. Xu, L. Wang. *Biosens. Bioelectron.*, 2015, **68**,204-209.
- 43 Y. Ma, S. Wang, L. Wang. *TrAC Trends Anal. Chem.*, 2015, **65**,13-21.
- 44 H. Li , L. Wang, *Analyst*, 2013, **138**, 1589-1595.
- 45 M. Deng, L. Wang, *Nano Res.*, 2014, **7**,782-793.
- 46 S. Lee, E.J.Cha, K. Park, and S.Y.Lee, et al., *Angew. Chem. Int. Ed.*, 2008, **47**, 2804-2807.
- 47 E. Dulkeith, A. C. Morteani, T. Niedereichholz, and T. A.Klar, et al., *Phys. Rev. Lett.*, 2002, **89**,  
203002-1-203002-4.
- 48 J. Deng, P. Yu, Y. Wang, and L. Yang, et al., *Adv. Mater.*, 2014, **26**, 6933-6943.
- 49 Y. Jiang, H. Zhao, Y. Lin, and N. Zhu, et al., *Angew. Chem. Int. Ed.*, 2010, **49**, 4800-4804.
- 50 Y. Jiang, H. Zhao, N. Zhu, and Y.Q. Lin, et al., *Angew. Chem. Int. Ed.*, 2008, **47**, 8601-8604.
- 51 L. Beqa, A. K. Singh, S. A. Khan, and D. Senapati, et al., *ACS Appl. Mater. Interfaces*, 2011, **3**,  
668-673.
- 52 S. Y. Lim, J. H. Kim, J. S. Lee, and C. B. Park, *Langmuir*, 2009, **25**, 13302-13305.
- 53 F. Gao, Q. Ye, P. Cui, and L. Zhang, *J. Agric. Food Chem.*, 2012, **60**, 4550-4558.
- 54 F. Gao, P. Cui, X. Chen, and Q. Ye, et al., *Analyst*, 2011, **136**, 3973-3980.
- 55 F. Gao, Q. Ye, P. Cui, and X. Chen, et al., *Anal. Methods*, 2011, **3**, 1180-1185.
- 56 I. S. Lim, F. Gorolesk, D. Mott, and N. Kariuki, et al., *J. Phys. Chem. B*, 2006, **110**, 6673-6682.

- 1  
2  
3 57 R. Jin, G. Wu, Z. Li, and C. A. Mirkin, et al., *J. Am. Chem. Soc.*, 2003, **125**, 1643-1654.  
4  
5 58 Y. F. Huang, and H. T. Chang, *Anal. Chem.*, 2006, **78**, 1485-1493.  
6  
7 59 R. W. Sabnis, *Handbook of Biological Dyes and Stains: Synthesis and Industrial Applications*,  
8 John Wiley @Sons, Inc., Hoboken, New Jersey, 2010, P60.  
9  
10 60 L. Stryer, *Annual Rev. Biochem.*, 1978, **47**, 819-846.  
11  
12 61 D. Zhao, W. H. Chan, Z. He, and T. Qiu, *Anal. Chem.*, 2009, **81**, 3537-3543.  
13  
14 62 K. E. Sapsford, L. Berti, and I. L. medintz, *Angew. Chem. Int. ed.*, 2006, **45**, 4562-4588.  
15  
16 63 A.P.Silva, H.Q.N.Gunaratne, T. Gunnlaugsson, and A.J.M.Huxley, et al., *Chem. Rev.*, 1997, **97**,  
17 1515-1566.  
18  
19 64 J. P. Rosa, J. C. Lima, P. V. Baptista, *Nanotech.*, 2011, **22**, 415202.  
20  
21  
22  
23  
24  
25  
26  
27  
28  
29  
30  
31  
32  
33  
34  
35  
36  
37  
38  
39  
40  
41  
42  
43  
44  
45  
46  
47  
48  
49  
50  
51  
52  
53  
54  
55  
56  
57  
58  
59  
60